

A Comparative Study over Degradation of Direct Green 6 by using Synthesized Magnesium Aluminate and Magnesium Zincate Nanoparticles

Shilpa G¹, Yogendra K¹, Mahadevan K.M², Madhusudhana N¹ and Santhosh A.M¹

*1*Department of P. G. Studies and Research in Environmental Science, Kuvempu University, Jnana sahyadri, Shankaraghatta, Shivamogga, Karnataka, India

2 Department of P. G Studies and Research in Chemistry, P.G. Centre Kadur, Kuvempu University, Kadur (T), Chickmagalur (D), Karnataka, India

Abstract: Magnesium Aluminate ($MgAl_2O_4$) and Magnesium Zincate ($MgZnO_4$) nanoparticles were synthesized by solution combustion method, which were used as photocatalyst for the degradation of water containing direct green 6 (DG6). These synthesized nanoparticles were characterized by X-ray diffraction (XRD), scanning electron microscope (SEM), UV-absorption spectroscopy and FT-IR spectra studies. It was calculated that the corresponding band gap was found to be 2.9eV and 3.07eV respectively and also average crystalline size was found to be 13nm and 28nm. Photocatalytic degradation was determined against DG6 by varying parameters such as, catalyst concentration, pH, and dye concentration. From these experimental results we know that, the maximum degradation was found to be 97.99% for $MgAl_2O_4$ nanoparticle and 94.64% for $MgZnO_4$ nanoparticle. Hence the efficiency of photodegradation of DG6 dye by using $MgAl_2O_4$ and $MgZnO_4$ nanoparticles was ascertained.

Key Words: Direct Green 6, $MgAl_2O_4$, $MgZnO_4$, degradation.

Date of Submission: 20-04-2018

Date of acceptance: 07-05-2018

I. Introduction

Dyes are the major sources for environmental contamination, these dyes are majorly used in textile industries and industrial waste water consists of these dyes, mainly azo dyes (1). More than 50% of textile dyes is azoic dyes which are recognized by nitrogen π -bound (2). Moreover, these azo dyes are non biodegradability due to their carcinogenicity, complex structure and high molecular weight (3). However, dyes are highly soluble in water contaminates water and also poisonous, this depletes water quality of water, but it also impacts on flora and fauna of water (4) and in developing countries (e.g., Bangladesh, West Bengal (India), Sri Lanka etc.) water bodies are highly polluted and causes environmental problems due to without any treatment of waste water (5). Direct green 6 (DG6), has diazo group, it has toxicity and carcinogenic nature (6). In the earlier studies other researcher have investigated the degradation of DG6 by different nanoparticles such as, Sr and Ag co-doped TiO_2 , nano-strontium titanate (7) (8) and also removal of dye from activated carbon prepared by agro waste Traditional treatment methods are not able to remove complete colour from the waste water due to their aromatic groups in dye, but it can transfer pollutants from one phase to another phase, these methods are inefficient and costly. But in recent years, researcher has developed advance oxidant process (AOPs) to eliminate or destruction of dyes in aqueous medium. Some of the AOPs are Fenton reaction, ozonation, sonophotocatalysis, electro-chemical oxidation and heterogeneous photocatalysis (9). Among these heterogeneous photocatalysis is an effective tool for destroy dyes present in waste water (10). Out of these methods heterogeneous photocatalysis has emerged as a very efficient tool for the eradication and mineralization of dyes (11). In photocatalysis, light energy from a light source excites an electron from the valence band of the catalyst to the conduction band with a series of reactions which results in the formation of hydroxyl radicals. The hydroxyl radicals have high oxidizing potential and therefore can attack most organic structures causing oxidation. However, this method is cost effective and doesn't produce any secondary pollutants (12).

In our studies mainly focused on the photocatalytic degradation of direct green 6 dye by using synthesized magnesium aluminate and magnesium zincate nanoparticles and effect of pH, dye concentration and the catalyst concentration were studied.

II. Experimental

2.1. Materials:

The commercially available water soluble dyes Direct Green 6 were obtained from Panam Biochemicals, Bangalore and used without further purification. Its structure is given in Fig. 1. The chemicals Magnesium Nitrate ($Mg(NO_3)_2$), Zinc Nitrate ($Zn(NO_3)_2 \cdot 6H_2O$), AR, Aluminium Nitrate ($Al(NO_3)_3 \cdot 9H_2O$) were obtained from Loba Chemicals, Mumbai and Glycine ($C_2H_5NO_2$) were obtained from Hi-Media Chemicals, Mumbai. Sodium hydroxide (LR, $\geq 97\%$), which are used for adjusting the pH of the dye solution, were procured from RFCL Limited, New Delhi. The visible spectrophotometer (Elico, SL 177) has been used for recording absorbance at 493nm (λ_{max}). Later the absorbance with respect to time was recorded by visible spectrophotometer (Elico, SL 177).

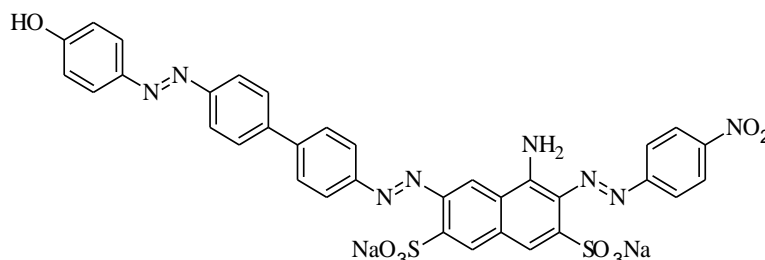


Fig 1: Chemical structure of Direct Green 6

2.2. Synthesis of Nanoparticles: The synthesis of Magnesium Aluminate and Magnesium Zincate nanoparticles by simple solution combustion method using glycine as a fuel.

2.2.1. Synthesis of $MgAl_2O_4$ nanoparticles:

The $MgAl_2O_4$ nano-particle was prepared by solution combustion method using $Mg(NO_3)_2$, $Al(NO_3)_3 \cdot 9H_2O$ and $C_2H_5NO_2$ (as fuel). Initially, $Mg(NO_3)_2$, $Al(NO_3)_3 \cdot 9H_2O$ and $C_6H_{12}O_6$ were dissolved in 2:2:3 molar ratio with minimum quantity of water in a silica crucible. The crucible was introduced to the pre heated muffle furnace then furnace rises as heat from room temperature to $600^\circ C$. The solution boils and undergoes dehydration followed by decomposition along with the release of the certain amount of gases, it swells forming foam which ruptures with a flame. The product formed after combustion is a voluminous and foamy $MgAl_2O_4$. After the complete combustion, the crucible was taken out and allowed to cool.

2.2.2. Synthesis of $MgZnO_4$ nanoparticles:

The $MgZnO_4$ nano-particle was prepared by solution combustion method using $Mg(NO_3)_2$, $Zn(NO_3)_2 \cdot 6H_2O$, and $C_2H_5NO_2$ (as fuel). Initially $Mg(NO_3)_2$, $Zn(NO_3)_2 \cdot 6H_2O$ and $C_2H_5NO_2$ were dissolved in 2:2:3 molar ratio with minimum quantity of water in a silica crucible. The crucible was introduced to the pre heated muffle furnace then furnace raises as heat from room temperature to $600^\circ C$. The solution boils and undergoes dehydration followed by decomposition along with the release of the certain amount of gases, it swells forming foam which ruptures with a flame. The product formed after combustion is a voluminous and foamy $MgAl_2O_4$. After the complete combustion, the crucible was taken out and allowed to cool. [13]

2.3. Characterization of Synthesized Nanoparticle

2.3.1. X-Ray Diffraction (XRD):

The XRD patterns of $MgAl_2O_4$ and $MgZnO_4$ nanoparticles reveal that, the presence of orthorhombic and Hexagonal structure and the 2θ peaks were observed which related to Magnesium Aluminium, (23.17° , 29.42° , 36.73° , 44.46° , 64.97°) (JCPDS card No.01-075-0278) for $MgAl_2O_4$ and for $MgZnO_4$ the peaks were related to Magnesium Zinc (34.54° , 36.2° , 47.82° , 68.02° , 78.30°) (JCPDS card No.03-065-4596) and the XRD was performed by powder X-ray diffraction (Rigaku diffractometer) using Cu-K α radiation (1.5406 \AA) in a θ - 2θ configuration. The pattern obtained from the XRD analysis of the prepared $MgAl_2O_4$ and $MgZnO_4$ nanoparticles is presented in Figure 2a and 2b.

According to the Debye Scherrer's formula: $D = K\lambda/\beta \cos\theta$ (4)

In the present work, the powdered sample of newly synthesized $MgAl_2O_4$ and $MgZnO_4$ nanoparticles were examined by XRD studies and found that $MgAl_2O_4$ nanoparticle size varies from 4 nm to 24 nm and henceforth the average crystallite size was found to be 13 nm. Whereas $MgZnO_4$ nanoparticles found to be varied from 22 nm to 35 nm and its average size was achieved on 28 nm respectively.

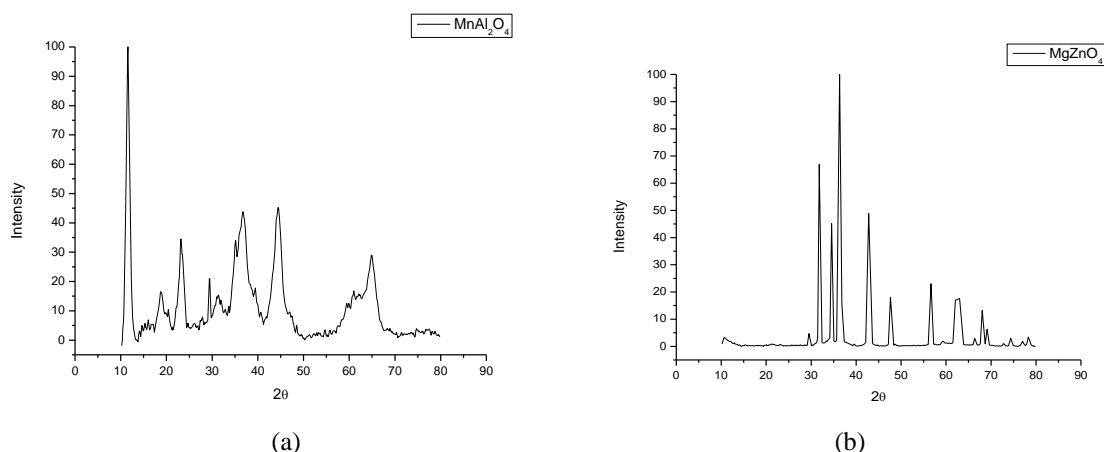


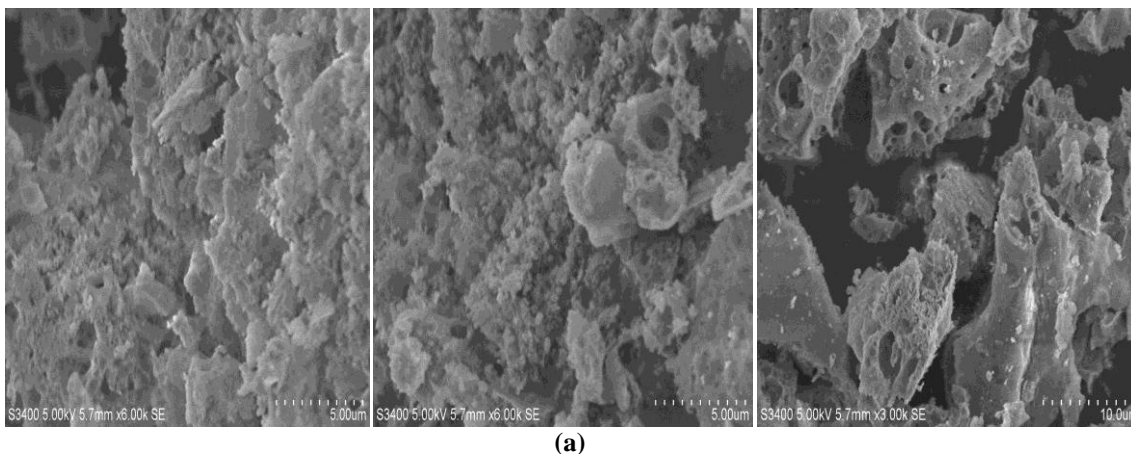
Fig 2: XRD of the synthesized Nanoparticles (a) $MgAl_2O_4$ (b) $MgZnO_4$

2.3.2. Scanning Electron Micrograph (SEM)

In the present study powdered sample of $MgAl_2O_4$ and $MgZnO_4$ nanoparticles were examined by using SEM technique for the study of external morphology of nanoparticles.

SEM study of $MgAl_2O_4$:

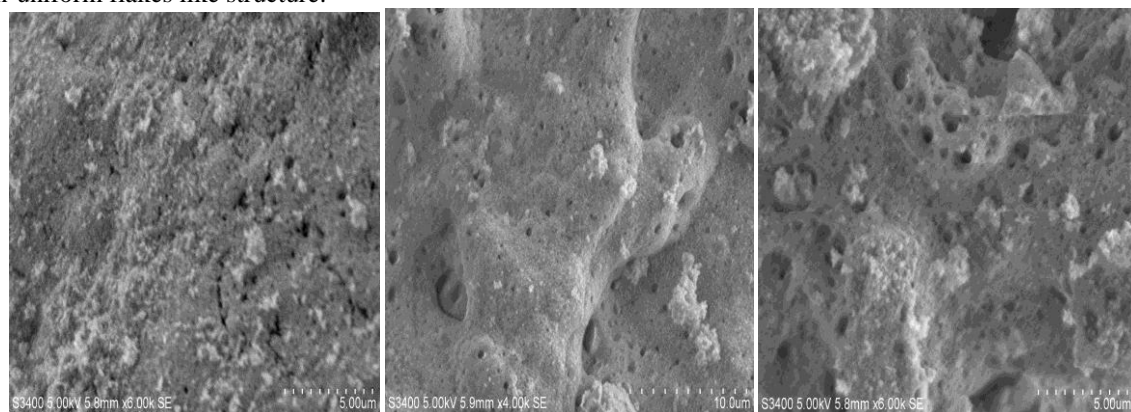
The SEM images of prepared $MgAl_2O_4$ nanoparticles exhibited irregular, dense crystals like appearance and non-uniform flakes like structure



(a)

SEM study of $MgZnO_4$:

The SEM images of prepared $MgZnO_4$ compound exhibited irregular, dense uniform cluster like appearance and non-uniform flakes like structure.



(b)

Fig 3: Scanning Electron Micrographs of synthesized (a) $MgAl_2O_4$ (b) $MgZnO_4$

2.3.3. UV-Vis Absorption Spectroscopy

The absorption spectrum of synthesized $MgAl_2O_4$ and $MgZnO_4$ nanoparticles were recorded using UV-VIS spectrophotometer of make Ocean Optics DH-2000, as taking synthesized nanoparticles directly into the spectroscopy over the wavelength range 200-1200nm. The spectral data showed the strong cut off appears at 424.19nm for $MgAl_2O_4$ and 403.39nm for $MgZnO_4$ [14, 15]. The band gap energy of the nanoparticles was calculated using the Planck's equation $E = hc/\lambda$ -- (Eq. 5) where h =Planck's constant, c =velocity of light and λ =wavelength. It was noticed that the band gap energy of nanoparticles was found to be 2.92eV for $MgAl_2O_4$ and 3.07eV for $MgZnO_4$. The UV-absorbance spectra of synthesized $MgAl_2O_4$ and $MgZnO_4$ are presented in Figure 4a and 4b.

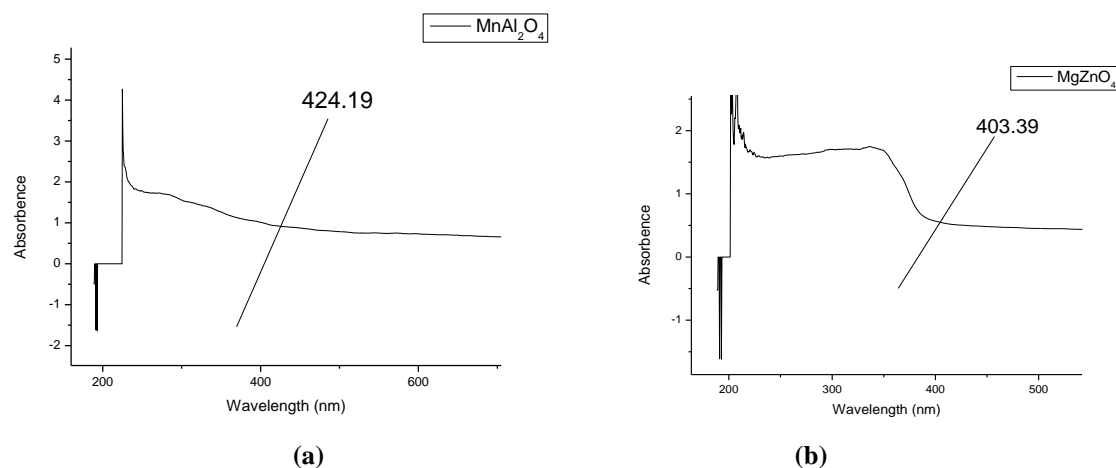
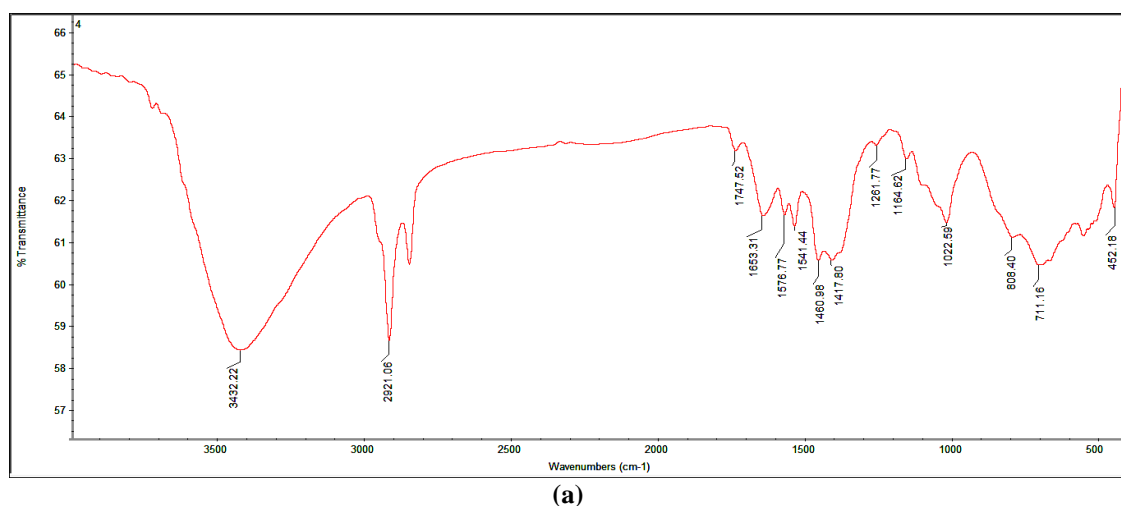
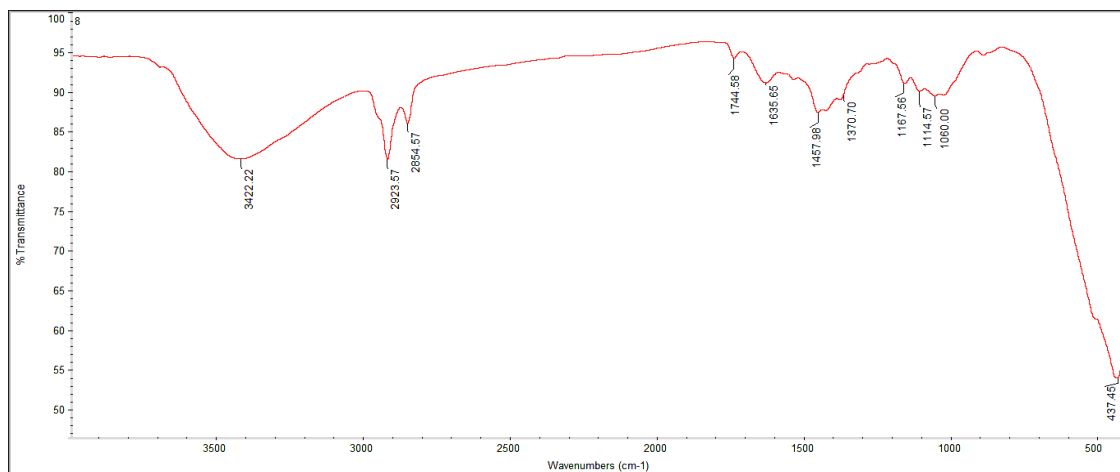


Fig 4: UV-absorption spectra of synthesized Nanoparticles (a) $MgAl_2O_4$ (b) $MgZnO_4$

2.3.4. FT-IR Spectroscopy

Fig: 5 showed the infrared spectrum of the synthesized nanoparticle such as $MgAl_2O_4$ and $MgZnO_4$ were ignited at 600°C. When these nanoparticles ignited while synthesis the absorption peaks are centred at 3432.22 cm^{-1} was assigned to the O-H stretching band and the band 1460.98 cm^{-1} was O-H bending band of $MgAl_2O_4$ are featured. Respectively $MgZnO_4$ nanoparticles absorption peaks are centred at 3432.22 cm^{-1} was assigned to the O-H stretching band and the band 1457.98 cm^{-1} was O-H bending band. These bands are the evidence for the presence of water in prepared nanoparticle. However, the strong peak observed at 711.16 cm^{-1} and 437.45 cm^{-1} were assigned to Mg-Al-O and Mg-Zn-O stretching band respectively, which indicating the presence of $MgAl_2O_4$ and $MgZnO_4$ nanoparticle in ignited compound [16].





(b)
Figure 5: FT-IR Spectra of synthesized (a) MgAl₂O₄ (b) MgZnO₄ nanoparticles

2.4. Experiment Procedure:

The experiments were conducted in presence of sunlight. Primarily 30ppm of DG6 dye solution was prepared by dissolving 0.03 g of dye with 1000ml double distilled water and transferred to glass reactors for further proceedings. Aqueous photocatalyst dispersion was prepared by adding catalyst dosages (0.1g to 0.6g) to a 100ml dye concentrations. Prior to irradiation, the solution were magnetically stirred in darkness for 2 to 3 min to establish adsorption equilibrium. Irradiation was carried under natural sunlight between 11 a.m. and 2 p.m. and the average intensity of sunlight during this period is 892×100 lux unit using lux meter. To study the reaction of different pH level (pH 3 to pH 12), the initial pH of the dye solution was adjusted by addition of NaOH solution. Here for pH media experiment catalyst dosage remains optimum. Further, the experiments were repeated at optimum catalyst dosage for the study of different dye concentration solution. At each 30-minute interval of irradiation time, a 5-ml of sample was taken, centrifuged and concentration of Direct Green 6 was monitored spectrophotometrically by recording absorbance of the supernatant at a wavelength of 493nm (λ_{max}).

The percentage was calculated by equation,

The percentage of decolourization = [(A₀ - A_t) ÷ A₀] × 100

Where, A₀ is the initial absorbance of the dye solution A_t is absorbance at time interval 't'

Mechanism of Photodegradation



Step 1: The nanoparticles under sunlight irradiation get excited and transfer electrons to the conduction band.



Step 2: It can reduce molecular oxygen and produce the super oxide radical.



Step 3: Molecular oxygen, adsorbed on the surface of the photocatalysts prevents the hole-electron pair recombination process [17, 18]. Recombination of hole-electron pair decreases the rate of photocatalytic degradation. This radical may form hydrogen peroxide or organic peroxide in the presence of oxygen and organic molecule.



Step 4: Hydrogen peroxide can be generated in another path.



Step 5: Hydrogen peroxide can form hydroxyl radicals which are powerful oxidizing agents.



Step 6: The radicals produced are capable of attacking dye molecules and degrade them.

III. Results and Discussions

3.1. Effect of Catalyst Concentration:

The effect of catalyst concentration was study by varying the catalyst concentration range from 0.1g to 0.6g/100ml of DG6 dye. The experimental results illustrated that, the efficiency of MgAl₂O₄ nanoparticles record 95.31% for 0.4g in 90min and for MgZnO₄ shows 92.18% for 0.5g in 90min (Fig.6). The highest

photocatalytic degradation shows in MgAl_2O_4 when compare to MgZnO_4 nanoparticles. Beyond the optimum catalyst concentration increase in the amount of catalyst which increases the number of dye molecules adsorbed on the dye surface and above catalyst concentration i.e. 0.4g for MgAl_2O_4 and 0.5g for MgZnO_4 nanoparticles was decreased in the photocatalytic degradation due to the overcrowding and collision of nanoparticles. However, the degradation was decreased due to the light penetration to the suspension (19).

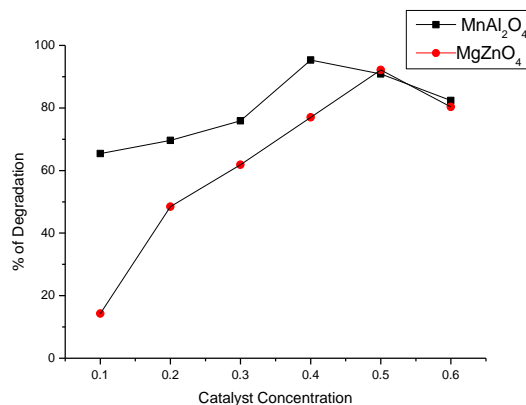


Fig 6: Effect of catalyst concentration on the photocatalytic degradation of DG6

3.2. Effect of pH: The pH parameter plays an important role in the degradation and pH varies from 3 to 11. The percentage of degradation of DG6 dye for MgAl_2O_4 (Fig. 7) increased from 75.66% to 97.99% from pH 3 to pH 10 and decreased to 97.76% at pH 11 in 90 minutes for 0.4g/100ml. For MgZnO_4 (Fig. 7) the percentage of degradation of the DG6 increased from 65.17% to 94.64% from pH 3 to pH 10 and decreased 80.13% at pH 11 in 90 minutes for 0.5g/100ml. From experimental results, the MgAl_2O_4 nanoparticles record maximum degradation when compared to MgZnO_4 nanoparticles due to the interaction of DG6 dyes on the surface of the catalyst increasing the generation of OH^\bullet radicals. These OH^- ions will generate more $\bullet\text{OH}$ radicals by combining with the hole of the semiconductor and the OH^\bullet radicals are the main oxidizing species responsible for photocatalytic degradation. After the optimum pH (above pH 10) the degradation efficiency was decreased, can be explained on the basis of amphoteric nature of the catalyst. Here the catalyst surface becomes negatively charged for higher pH value, which causes the electrostatic repulsion between the catalyst and negatively charged dyes [20]. The maximum percentage of degradation for the two different nanoparticles was achieved at pH 10. The alkaline condition is more suitable when compared to acidic condition as it gives effective and good results in smaller dosages of catalyst (21, 22, 23).

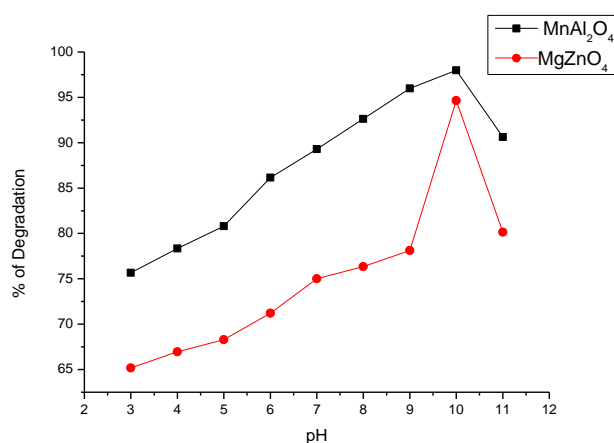


Fig 7: Effect of pH on the photocatalytic degradation of DG6

3.3. Effect of Initial Dye Concentration:

Dye concentration is a very important parameter in treatment of waste water. The effect of initial concentration of dye on the degradation was performed by varying the initial dye concentration from 30ppm to 50ppm with constant catalyst loading and pH. The results obtained for MgAl_2O_4 (Fig. 8) was 97.99% for 30ppm, 85.71% for 40ppm and 72.99% for 50ppm. And for MgZnO_4 (Fig. 8) is 94.64% for 30ppm, 83.25% for 40ppm and 69.86% for 50ppm, these experiments illustrated that the degradation efficiency was directly affected by the concentration.

When the concentration of the dye solution increases, this leads to the amount of dye adsorbed on the catalyst surface increases and affects the photocatalytic activity of the MgAl_2O_4 and MgZnO_4 nanoparticles, this also decreases the path length of photons entering into the dye solution. The degradation is mainly related to the formation of OH radicals, these OH radicals are the main critical species in the degradation process and The path length of photons entering the solution decreases, and in low concentration the reverse effect is observed, the number of photon absorption by the surface of catalyst in lower concentration when increase the dye concentration. Hence, the rate of degradation decreases with increase in the dye concentration (24, 25, 26, 27).

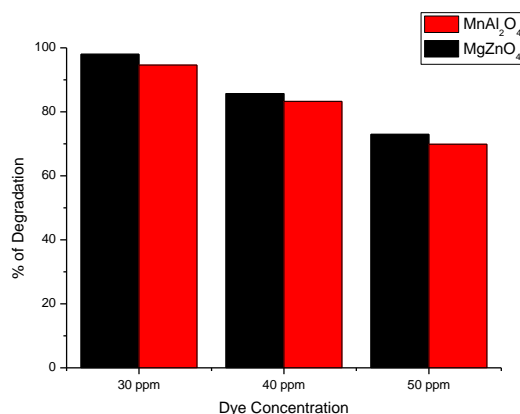


Fig 8: Effect of initial dye concentration on the photocatalytic degradation of DG6

IV. Conclusion

In the present study mainly focused on the degradation of DG6 dye under natural sunlight by synthesized MgAl_2O_4 and MgZnO_4 nanoparticles. The degradation depends on the size and band gap of the nanoparticle, MgAl_2O_4 nanoparticles achieved maximum degradation (97.99%) at 0.4g/100ml for pH 10 and for MgZnO_4 nanoparticles (94.64%) at 0.5g/100ml for pH 10 in a short interval time (90 min). Hence this can apply to the industry for the efficient treatment of the effluent which is hazardous to the environment and it is cost-effective too.

Acknowledgments

The authors thank the Department of P G Studies and Research in Environmental Science, Kuvempu University, Shankaraghatta, Shimoga, Karnataka, India for providing facilities to carrying out this research work.

References

- [1]. Moradi, S., Aberoomand-Azar, P., Raeis-Farshid, S., Abedini-Khorrami, S., and Givianrad, M.H, The effect of different molar ratios of ZnO on characterization and photocatalytic activity of TiO_2/ZnO nanocomposite, *Journal of Saudi Chemical Society*, (2016); 20, 373–378.
- [2]. Karimi, L., Zohoori, S., and Yazdanshenas, M.E, Photocatalytic degradation of azo dyes in aqueous solutions under UV irradiation using nano-strontium titanate as the nanophotocatalyst, *Journal of Saudi Chemical Society*, (2014); 18, 581–588.
- [3]. Alahiane, S., Sennaoui, A., Sakr, F., Qourzal, S., Dinne, M., and Assabbane, A, A study of the photocatalytic degradation of the textile dye Reactive Yellow 17 in aqueous solution by TiO_2 -coated non-woven fibres in a batch photoreactor, *Journal Materials and Environmental Science*, (2017) ; 8(10): 3556-3563.
- [4]. Hassaan, M.A., Nemr, A.E., and Madkour, F.F, Testing the advanced oxidation processes on the degradation of Direct Blue 86 dye in wastewater, *Egyptian Journal of Aquatic Research*, (2017); 43, 11–19.
- [5]. Habib, A.MD., Ismail, I.I.M., Mahmood, A.J., and Ullah, R.MD, Photocatalytic decolorization of Brilliant Golden Yellow in TiO_2 and ZnO suspensions, *Journal of Saudi Chemical Society*, (2011); 16, 423–429. doi:10.1016/j.jscs.2011.02.013
- [6]. Geetha, K., Velmani, N., Karthikeyan, S., and Shabudeen, S, Comparison on Equilibrium and Kinetic Studies on the Removal of Direct Green 6 from Aqueous Solutions using Activated Carbons prepared from Agro Waste, *Digest Journal of Nanomaterials and Biostructures*, (2016); 11(1), 199-212.
- [7]. Naraginti, S., Thejaswini, T.V.L., Prabhakaran, D., Sivakumar, A., Satyanarayana, V.S.V., and Prasad, A.S.A, Enhanced, Photocatalytic Activity of Sr and Ag co-doped TiO_2 Nanoparticles for the degradation of Direct Green-6 and Reactive Blue-160 under UV & visible light, *Spectrochimica Acta Part A : Molecular*, (2015); 149, 571-579.
- [8]. Ertugay, N., and Acar, F.N, Removal of COD and color from Direct Blue 71 azo dye wastewater by Fenton's oxidation: Kinetic study, *Arabian Journal of Chemistry*, (2017); 10, S1158–S1163.
- [9]. Kaur, J., and Singhal, S, Facile synthesis of ZnO and transition metal doped ZnO nanoparticles for the photocatalytic degradation of Methyl Orange, *Ceramic International*, (2014); 40(5), 7417-7424. doi.org/10.1016/j.ceramint.2013.12.088.
- [10]. Barka, N., Qourzal, S., Assabbane, A., Nounah, A., and Ait-Ichou, Y, Photocatalytic degradation of an azo reactive dye, Reactive Yellow 84, in water using an industrial titanium dioxide coated media, *Journal of Saudi Chemical Society*, (2010); 3, 279–283.
- [11]. Sangari, N. U., & Velusamy, P, Photocatalytic Decoloration Efficiencies of ZnO and TiO_2 : A Comparative Study, *Journal of Environmental Science and Pollution Research*, (2016); 2(1), 42–45.
- [12]. Kamel, M. M., Mashaly, H. M., and Abdelghaffar, F, Photocatalyst Decolorization of Reactive Orange 5 Dye Using MgO Nano Powder and H_2O_2 Solution, *World Applied Sciences Journal*, (2013); 26(8), 1053–1060.
- [13]. Madhusudhana. N, Yogendra. P and Mahadevan K. M, Photocatalytic Decolorization of Textile Effluent by using Synthesized Nano particles, *J. Environ. Nanotechnol*, (2014); Vol. 3(4), 41-53.

- [14]. Jayamadhava, P., Sudhakara, A., Ramesha, S., & Nataraja, G. Synthesis of ZnO nano particle as an alternative catalyst for Photocatalytic degradation of brilliant red azo dye, *American Journal of Environmental Protection*, (2014); 3(6), 318–322.
- [15]. Shilpa G, Yogendra K, Mahadevan K. M, Madhusudhana N, Synthesis of ZnAl₂O₄ Nano-Particles and Its Application for Photo-Catalytic Decolourization of Model Azo Dye Acid Red 88 in Presence of Natural Sunlight *Journal of Applied Chemistry*, (2017), 10, 35-41.
- [16]. Chandrappa K. G, Venkatesha T. V, Nayana K.O. and Punithkumar M. K., Generation of nanocrystalline NiO particles by solution combustion method and its Zn-NiO composite coating for corrosion protection, *J. Materials and Corrosion*, (2012); 63, 445-455.
- [17]. Madhusudhana N, Yogendra K, Mahadevan K. M, Santhosh A. M, Study on photocatalytic degradation coralene red f3bs by using synthesized Al₂O₃ nanoparticles, *AGU International Journal of Engineering & Technology*, (2018); 6, 29-37.
- [18]. Santhosh, A.M., Yogendra, K., Mahadevan, K.M., & Madhusudhana. N, Photodegradation of Congo red azo dye, a Carcinogenic Textile dye by using synthesized Nickel Calcite Nanoparticles, *International Journal of Advance Research in Science and Engineering*, (2017); 6(7), 51-64.
- [19]. Krishnakumar, B., & Swaminathan, M, Solar photocatalytic degradation of Acid Black 1 with ZnO, *Indian Journal of Chemistry*, (2010); 49, 1035–1040.
- [20]. Sakthivel, S., Neppolian, B., Shankar, M.V., Arabindoo, B., Palanichamy, M., and Murugesan, V, Solar photocatalytic degradation of azo dye : comparison of photocatalytic efficiency of ZnO and TiO₂, *Solar Energy Materials & Solar Cells*, (2003); 77, 65–82.
- [21]. Guillard, C., Lachheb, H., Houas, A., Ksibi, M., Elaloui, E., and Herrman, J.M, Influence of chemical structure of dyes of pH and of inorganic salts on their photocatalytic degradation by TiO₂ Comparison of efficiency of powder and supported TiO₂, *Journal of Photochemistry and Photobiology A: Chemistry*, (2003); 158, 27-36.
- [22]. Mehta, R., and Surana, M, Comparative study of photo-degradation of dye Acid Orange -8 by Fenton reagent and Titanium Oxide-A review, *Der Pharma Chemica*, (2012); 4(1), 311–319.
- [23]. Turchi, C.S., and Ollis, D.F. Photocatalytic Degradation of Organic Water Contaminants: Mechanisms Involving Hydroxyl Radical Attack, *Journal of Catalysis*, (1990); 122, 178-192.
- [24]. Neppolian, B., Choi, H. C., Sakthivel, S., Arabindoo, B., & Murugesan, V, Solar light induced and TiO₂ assisted degradation of textile dye reactive blue, *Chemosphere*, (2002); 4, 1173–1181.
- [25]. Jayant Dharma, Aniruddha Pisal and PerkinElmer, Inc., Application note: UV/Vis/NIR spectrometer (2009).
- [26]. Habib, A., Shahadat, T., Bahadur, N. M., Ismail, I. M. I., & Mahmood, A. J, Synthesis and characterization of ZnO-TiO₂ nanocomposites and their application as photocatalysts, *International Nano Letters*, (2013); 3(5), 1–8.
- [27]. Natarajan, K., Natarajan, T.S., Bajaj, H.C., & Tayade, R. J, Photocatalytic reactor based on UV-LED / TiO₂ coated quartz tube for degradation of dyes, *Chemical Engineering Journal*, (2011); 178, 40–49.

IOSR Journal of Applied Chemistry (IOSR-JAC) is UGC approved Journal with Sl. No. 4031, Journal no. 44190.

Shilpa G "A Comparative Study over Degradation of Direct Green 6 by using Synthesized Magnesium Aluminate and Magnesium Zincate Nanoparticles." *IOSR Journal of Applied Chemistry (IOSR-JAC)* 11.5 (2018): 01-08.